IOWA STATE UNIVERSITY
Digital Repository

Graduate Theses and Dissertations

Iowa State University Capstones, Theses and Dissertations

2010

Design and synthesis of mixed oxides nanoparticles for biofuel applications

Senniang Chen
Iowa State University

Follow this and additional works at: https://lib.dr.iastate.edu/etd

Part of the Chemistry Commons

www.manaraa.com

Design and synthesis of mixed oxides nanoparticles for biofuel applications

by

Senniang Chen

A thesis submitted to the graduate faculty

in partial fulfillment of the requirements for the degree of

MASTER OF SCIENCE

Major: Chemistry

Program of Study Committee:
Victor Shang-Yi Lin, Co-major Professor
Marek Purski, Co-major Professor
Ning Fang

Iowa State University

Ames, Iowa

2010

TABLE OF CONTENTS

ABSTRACT

The work in this dissertation presents the synthesis of two mixed metal oxides for biofuel applications and NMR characterization of silica materials. In the chapter 2, high catalytic efficiency of calcium silicate is synthesized for transesterfication of soybean oil to biodisels. Chapter 3 describes the synthesis of a new Rh based catalyst on mesoporous manganese oxides. The new catalyst is found to have higher activity and selectivity towards ethanol. Chapter 4 demonstrates the applications of solid-state Si NMR in the silica materials.

CHAPTER 1. INTRODUCTION

This dissertation begins with chapter 1, which gives a general introduction of mixed oxides used as heterogeneous catalyst in bioethanol application. Chapter 2 describes the synthesis of calcium oxides for transesterfication of soybean oil. Chapter 3 presents a new catalyst, Rh based on mesoporous manganese oxides, for selective production of ethanol from syngas. Chapter 4 shows the solid-state Si NMR applied in characterization of the inorganic materials. The Si NMR can be used to calculate the Ca/Si ratio in the MCS materials and the concentration of organic functional group on the MSN.

Introduction

Besides the depletion of oil reserves, fossil fuel usage also creates environmental pollution. The main pollutants come from the vehicle emission, which includes sulfur and nitrogen oxides, carbon monoxide and suspended fine particles. Among those, the nitrogen oxides can create a secondary pollution by interacting with hydrocarbon and sunlight, which leads to the formation of ozone in the troposphere. The suspended fine particles, precursors of ozone and acid deposition can cause air pollution as well as ecosystem degradation. The combustion of fossil fuel also adds greenhouse gas to the atmosphere, which is blamed for the global warnings. The fossil fuel usage can really threaten both human health and environment, thus a nontoxic and environment friendly fuel is needed.

Ever since the oil crisis, people are searching for alternative energy sources. Biomass becomes an important candidate because it is renewable, biodegradable, and nontoxic.

Biomass is organic material derived from natural sources, such as agricultural crops and residues, wood and its residules.[1]Biomass can be converted into a wide range of biofuels. Comparing to the fossil fuel, biofuel is clean and environmental friendly. It contains insignificant amount of sulfur. Besides, unlike the fossil fuel emission, the biofuel emission does not increase the concentration of greenhouse gases because the carbon is derived from the biomass, which originally comes from the atmosphere. This also makes biomass renewable.

One important member of the biofuel family is bioethanol. Ethanol is known to be a fuel additive, which attracts more and more attention these days. The most common way of producing ethanol is fermentation of sugars from corn grain and sugar cane. There are several drawbacks of this method. First, the supply of the raw materials such as corn grain and sugar cane, is expected to be limited in the near future.[3] Second, production of pure ethanol is expensive because it required energy-intensive distillation step, although the process of fermentation is commercially practical. Third, some biomass such as hemicellulose and cellulose, need chemical and physical treatment and enzymatic breakdown of the macromolecules before the fermentation.[4] Finally, the microorganisms can not completely metabolize the pentose sugars and hexose sugars, which precludes the application of the fermentation of the sugars derived from lignocellulose or woody biomass.[3, 5]

In contrast to the fermentation method, the gasification of entire biomass component into syngas followed by catalytic conversion of syngs to liquid fuels is known to be a promising way to convert biomass into liquid fuels.[6] In the gasification process, the biomass reacts with air or oxygen and followed by steaming to produced syngas.[7] Syngas is a mixture

gas which contains mainly CO, H_2, CO_2 and H_2O. It could also contain some other components such as, NH_3, H_2S and CH_4.

Mixed metal oxides are used as heterogeneous catalysts to convert syngas into liquid fuel and chemicals. They include noble metals based catalysts, Fischer-Tropsch type catalysts, methanol synthesis catalysts and Mo-based catalysts. [5, 7]

The traditional Fischer-Tropsch type catalysts are Fe, Co, Ni or Ru metal on SiO_2 or Al_2O_3 support. The Fischer-Tropsch catalysts can promote the carbon chain growth, thus are used to synthesize long-chain hydrocarbons and oxygenates from the syngas. In order to improve the catalytic performance, the Fisher-Tropsch catalyst can be modified in many ways, e.g., by adding a promoter or using various supports. The most commonly used promoters are transition metal oxides such as TiO_2 and MnO_2, and alkali metals such as K, Cs and Na.[5, 8, 9] For example, small amount of TiO_2 added to the silica supported Co catalyst results in significant increase of the dispersion of Co and the Co surface area.[9] CeO_2 is used to support Co, which increases the selectivity towards C5+.[10] The supports used to modify the catalysts include SiO_2, zeolite and carbon. The carbon support can increase the Co metal dispersion[11] and limit the surface mobility of the iron nanoparticles. [12] When the iron nanoparticles are immobilized on the carbon support, the agglomeration, which leads to a subsequent decrease of the catalyst performance over times, can be reduced. [12] Zeolite was used to support the Fisher-Tropsch type catalyst because of its acidity.[13] The TiO_2 support has also been reported.[14]

The methanol synthesis catalysts used in industry are ZnO/Cr_2O_3 and Cu/ZnO based catalyst.[5] It was found that alkali metal could promote these type of catalysts to synthesize higher alcohols.[15] It was reported that the effect of alkali promote Cu/MgO was in the order of Na>K>Rb>Li at the reaction condition of 433K and 5.0MP.[16] However, for Co and Cu based catalysts, Li could promote the catalyst for higher selectively towards higher alcohols and could make the catalysts more stable during the reaction.[17] Transition metals can also be added as promoter. It was reported that a Fe modified $CuMnZrO_2$ catalyst had highly dispersed Cu and Cu-Fe phase, which made it a good catalyst for synthesis of straight-chain alcohols.[18, 19]

The Mo based catalyst receives quite a lot of attention because of its resistance to sulfur poisoning syngas, which eliminates the need of cleanup of syngas containing H_2S. The Mo based catalyst can be divided into two categories, the unsulfided and sulfided. The sulfided Mo based catalyst, MoS_2, was studied extensively with H_2S rich syngas.[20] The alkali and transition metal oxides can promote Mo based catalyst for the synthesis of alcohols from syngas with high selectivity and reactivity. The Dow Chemical Company developed the first alkali doped Mo catalyst for synthesis of alcohols from syngas. The catalyst could produce 70~80% of alcohols and 15~30% hydrocarbons. Moreover, the C3+ alcohols products are mostly linear alcohols.[5, 21] It was further reported that Ni promoted alkali doped MoS_2 could decrease the selectivity of methanol from 52% to 11%.[22] Chemists also play with different supports besides SiO_2 such as zeolite[23], active carbon[24] and carbon nanotubes.[25, 26] It was noticed that the Mo/zeolite could reduce selectivity towards hydrocarbons and increase selectivity towards alcohols and carboxylic acids.[23] The unsulfided Mo based catalysts are

also investigated. Zaman synthesized K promoted MoP/SiO$_2$ with very low methane selectivity at 8% and very high selectivity of oxygenates. [27] K and Ni promoted beta Mo$_2$C catalyst was also used for higher alcohol synthesis. Although the beta Mo$_2$C produced mainly hydrocarbons, the addition of K and Ni could lead to a remarkable selectivity towards oxygenates. [28, 29 30]

The noble metals used to directly convert syngas into ethanol or higher alcohol include Rh,[31] Ru[32] and Re[33]. Rh is most commonly studied because it has highly selectivity towards ethanol.[5] Rh can adsorb CO both dissociatively and nondissociatively. The formation of higher oxygenations requires the CO to adsorb dissociately on Rh so that the alkyl chain can grow by stepwise addition of CH$_2$ units. The nondissociative adsorbed CO can insert at the end of the alky chain to form ethanol. [34]

The catalytic performance of the Rh based catalyst is affected by the promoter, support, and even the Rh precursor. The promoters used include alkali, transition and rare earth metals. The mechanisms are investigated by EPR, TPR, TPD, IR and XPS techniques. Wang pointed out that the Mn could exist as isolated Mn^{2+} ion and even form Rh-Mn mixed oxides to stabilize the Rh$^+$ species..[35] However, Trevino found that only the MnO particles, but not the Mn^{2+} ions, could promote the Rh catalyzed formation of ethanol and ethylacetate.[34] Nevertheless, it is well accepted that in order to promote the Rh, the promoter needs to have close interaction with Rh particles. Sometimes, two or more promoters are added to enhance the Rh catalytic performance. The Rh/SiO$_2$ catalyst doubly promoted with Mn and Li is the often used for ethanol synthesis from syngas. In the Rh-Mn-Li/SiO$_2$ catalyst,

the Li inhibited the formation of Rh-Mn mixed oxides and increase the Rh^0 concentration on the SiO_2 support. [35] It is also found that the La and V doubly promoted Rh/SiO2 showed nine times higher reactivity than the non-promoted ones, while La promoted Rh/SiO_2 and V promoted Rh/SiO_2 only had three times higher reactivity compared to the non-promoted ones. [36]

The materials used to support Rh catalyst are usually SiO_2, Al_2O_3, carbon and other metal oxides. The Rh based catalysts on weakly basic oxides support such as La_2O_3, Cr_2O_3, TiO_2 and ThO_2, and on the strongly basic oxides support such as MgO and ZnO generate methanol as major product. The Rh based catalysts on acidic support turns out to generate hydrocarbons. [5, 37] Pore structure and surface area are important in the gas reaction. The reaction can occur at the exterior and interior surface of the catalyst, and the rate of the reaction is a function of the surface area. The larger amount of accessible surface to the reactant results in faster reaction rate. Thus, it is customary to disperse metal catalyst on some porous support with high surface area such as mesoporous silica particle, high surface alumina and carbon support. [38] Among those, SiO_2 is the most commonly used support. It is found that SiO_2 not only can facilitate the dispersion of Rh particles, but the silica pores can limit the Rh particle size, which has great effect on the catalytic performance. [39] It was found that the Rh particles with size between 2 and 4 nm showed high activity in the formation of C2 oxygenations from syngas. [40] In addition, the morphology of the supports also plays a role. Among the investigated catalysts with three different types of carbon supports, the carbon nanotubes supported Rh-based catalyst had better catalytic performance than active carbon and mesoporous carbon (CMK-3) ones. [41, 42]

Finally, the precursor of the Rh can also change the catalytic performance. It is found that the chloride precursors are better than the nitrate ones. It is supposed that the chorine can improve the interaction between the Rh particles and Mn promoter and therefore improve the Rh particle geometries, size distributions and the ratio of Rh^+/Rh^0.[43]

This review highlights the great interest in employing mixed metal oxides catalyst in converting syngas into ethanol and higher alcohols. The current synthesis of ethanol and higher alcohol is feasible, but the conversion is not high enough for commercial applications. The improvement of the mixed oxides is needed for high reactivity and selectivity for ethanol and higher alcohols in this reaction.

Reference

1.   Krongkaew Laohalidanond*, J. H. a. C. W., *KMITL Sci. Tech. J.* **2007,** 6, (1), 6.

2.   Anton A. Kiss, F. O., Alexandre C. Dimian, and Gadi Rothenberg, *Topics in Catalysis* **2006,** 40, 10.

3.   Gray, K. A.; Zhao, L. S.; Emptage, M., *Current Opinion in Chemical Biology* **2006,** 10, (2), 141-146.

4.   Rostrup-Nielsen, J. R., *Science* **2005,** 308, (5727), 1421-1422.

5.   Subramani, V.; Gangwal, S. K., *Energy & Fuels* **2008,** 22, (2), 814-839.

6.   Huber, G. W.; Iborra, S.; Corma, A., *Chemical Reviews* **2006,** 106, (9), 4044-4098.

7.   Spivey, J. J.; Egbebi, A., *Chemical Society Reviews* **2007,** 36, (9), 1514-1528.

8.   Mirzaei, A. A.; Habibpour, R.; Faizi, M.; Kashi, E., *Applied Catalysis a-General* **2006,** 301, (2), 272-283.

9.   Hinchiranan, S.; Zhang, Y.; Nagamori, S.; Vitidsant, T.; Tsubaki, N., *Fuel Processing Technology* **2008,** 89, (4), 455-459.

10.   Shi, H. B.; Li, Q.; Dai, X. P.; Yu, C. C.; Shen, S. K. In *CeO2-promotion of Co/SiO2 Fischer-Tropsch synthesis catalyst*, 7th Natural Gas Conversion Symposium, Dalian, PEOPLES R CHINA, Jun 06-10, 2004; Bao, X.; Xu, Y., Eds. Elsevier Science Bv: Dalian, PEOPLES R CHINA, 2004; pp 313-318.

11.   D'Souza, L.; Jiao, L.; Regalbuto, J. R.; Miller, J. T.; Kropf, A. J., *Journal of Catalysis* **2007,** 248, (2), 165-174.

12.   Graham, U. M.; Dozier, A.; Khatri, R. A.; Bahome, M. C.; Jewell, L. L.; Mhlanga, S. D.; Coville, N. J.; Davis, B. H., *Catalysis Letters* **2009,** 129, (1-2), 39-45.

13.   Abramova, A. V.; Panin, A. A.; Kliger, G. A.; Kulikova, E. A.; Slivinsky, E. V. In *Production of synthetic fuels from alternative petroleum raw material by method of Fischer-Tropsch on zeolite catalysts*, 3rd Conference of the Federation-of-European-Zeolite-Association, Prague, CZECH REPUBLIC, Aug 23-29, 2005; Cejka, J.; Zilkova, N.; Nachtigall, P., Eds. Elsevier Science Bv: Prague, CZECH REPUBLIC, 2005; pp 1709-1716.

14.   Das, P. C.; Pradhan, N. C.; Dalai, A. K.; Bakhshi, N. N., *Fuel Processing Technology* **2004,** 85, (13), 1487-1501.

15.   Smith, K. J.; Anderson, R. B., *Canadian Journal of Chemical Engineering* **1983,** 61, (1), 40-45.

16.   Hu, B.; Yamaguchi, Y.; Fujimoto, K., *Catalysis Communications* **2009,** 10, (12), 1620-1624.

17.   de Aquino, A. D.; Cobo, A. J. G. In *Synthesis of higher alcohols with cobalt and copper based model catalysts: effect of the alkaline metals*, 4th European Congress on

Catalysis (EUROPACAT-IV), Rimini, Italy, Sep 05-10, 1999; Elsevier Science Bv: Rimini, Italy, 1999; pp 209-216.

18.   Xu, R.; Wei, W.; Li, W. H.; Hu, T. D.; Sun, Y. H., *Journal of Molecular Catalysis a-Chemical* **2005,** 234, (1-2), 75-83.

19.   Xu, R.; Yang, C.; Wei, W.; Li, W. H.; Sun, Y. H.; Hu, T. D., *Journal of Molecular Catalysis a-Chemical* **2004,** 221, (1-2), 51-58.

20.   Chen, A. P.; Wang, Q.; Li, Q. L.; Hao, Y. J.; Fang, W. P.; Yang, Y. Q., *Journal of Molecular Catalysis a-Chemical* **2008,** 283, (1-2), 69-76.

21.   Fang, K. G.; Li, D. B.; Lin, M. G.; Xiang, M. L.; Wei, W.; Sun, Y. H. In *A short review of heterogeneous catalytic process for mixed alcohols synthesis via syngas,* Symposium on Catalytic Synthesis and Utilization of Alcohols held at the 236th ACS National Meeting, Philadelphia, PA, Aug 17-21, 2008; Elsevier Science Bv: Philadelphia, PA, 2008; pp 133-138.

22.   Li, D. B.; Yang, C.; Li, W. H.; Sun, Y. H.; Zhong, B. In *Ni/ADM: a high activity and selectivity to C2+OH catalyst for catalytic conversion of synthesis gas to C-1-C-5 mixed alcohols,* Symposium on Syntheric Clean Fuels from Natural Gas and Coal-Bed Methane, New York, NY, Sep 07-11, 2003; Springer/Plenum Publishers: New York, NY, 2003; pp 233-239.

23.   Liu, S.; Gujar, A. C.; Thomas, P.; Toghiani, H.; White, M. G., *Applied Catalysis a-General* **2009,** 357, (1), 18-25.

24.   Li, Z. R.; Fu, Y. L.; Jiang, M.; Hu, T. D.; Liu, T.; Xie, Y. N., *Journal of Catalysis* **2001,** 199, (2), 155-161.

CHAPTER 2 CALCIUM SILICATE MIXED OXIDE-BASED HETEROGENEOUS CATALYSTS FOR BIODIESEL PRODUCTION

Abstract

A series of calcium silicate mixed oxides has been developed for biodiesel production. It has been shown that these materials can catalyze transesterification reactions from feedstock with various fatty acid contents. However, their reaction kinetics for biodiesel synthesis was very slow compared to the homogeneously catalyzed reactions. Herein, we report on the development of two types fast-reacting solid catalysts for biodiesel production: a non-porous catalyst and an anionic surfactant-templated catalyst. Both families of catalysts yielded much higher rates of transesterification reaction compared previously reported mesoporous calcium silicate catalysts. In addition, both the preparation time of catalysts and the cost of preparation were significantly reduced. Details of material synthesis and its effect on catalysis are discussed.

Keywords: Mixed oxides, calcium silicate materials, heterogeneous catalysts, biodiesel, transesterification

Introduction

Biodiesel, also known as Fatty Acid Methyl Esters (FAME), is one of the most promising alternative biofuels and is currently produced by a base-catalyzed transesterification reaction with triglycerides and methanol[1]. In such a process, triglycerides

react with alcohols, with the presence of sodium methoxide, sodium hydroxide, or potassium hydroxide, and transform into monoalkyl esters of fatty acids and glycerol [1]. In additional to alkyl esters and glycerol, water, soap, and unreacted strong base are also present in the mixture of products. Therefore, post-treatments such as neutralization, washing, and drying are needed after separation of glycerol [1]. Clearly, the neutralization processes increases the use and water, and necessitates of drying the biodiesel. Up to 4 litters of water are used in the post-treatment of every one litter of biodiesel produced, and vacuum drying of the product at elevated temperature is usually needed after the washing processes. Further, these homogeneous catalysts are not suitable for feedstock with high fatty acid content due to rapid saponification reaction which causes problems in the post-treatments of biodiesel.

Very recently, mesoporous calcium silicate catalysts have been reported to catalyze heterogeneous transesterification reactions [2]. The major advantage of these solid catalysts is that no energy-intensive post-treatments are needed. Also, it has been shown that the mesoporous calcium silicate family can work with soybean oil (SBO) as well as poultry fat (PF) which contains high free fatty acid content (~10%) [2]. The major disadvantage of the mesoporous calcium silicate catalysts is their slow reaction kinetics. They needed one to several days to convert SBO and PF into biodiesel.

In order to truly replace the homogeneous catalysts in the current production processes of biodiesel, we not only have to improve the reaction kinetics but take into consideration both cost-effectiveness and ease of preparation. In this article, we present the development of two systems of calcium silicate mixed oxide material for biodiesel production. In the first catalyst system, we fine tuned the experimental variables of the synthesis of calcium silicate materials and were able to improve the reaction kinetics

severalfold in converting SBO and PF into biodiesel. In the second system, we use an anionic surfactant, in contrast to the cationic surfactant, in mesoporous calcium silicate synthesis to prepare the materials. The reaction time for transesterification of the catalyst is 2 hours.

Experimental

2.1 Chemicals and Materials

Calcium oxide (CaO), Calcium hydroxide Ca(OH)$_2$, sodium hydroxide (NaOH), hydrogen chloride (HCl), methanol, and acetone were purchased from Fisher. Solid sodium silicate powder was provided by PQ Corporation. Cetyltrimethylammonium bromide (CTAB), tetraethylorthosilicate (TEOS), tetraethylene glycol, phosphorus oxychloride and 11-bromoundec-1-ene were purchased from Sigma-Aldrich. Degummed soybean oil and poultry fat were obtained from West Central.

2.2 Preparation of Solid Catalysts

2.2.1 Synthesis of Calcium Silicate (CS) Mixed Oxide Catalysts

The synthesis of materials was carried out under 80 °C and constantly stirring for 2 h followed by hot filtration. TEOS was introduced dropwise at 30 mL/h by a syringe pump. Calcium oxide powder was added gradually when the mixture turned cloudy which was about 3 min after the beginning of the introduction of TEOS. The as-synthesized materials were washed with copious amount of water and methanol. For materials that contained CTAB, calcination was applied for 6 h at 600 °C after lypholization. For those materials without CTAB, lypholized powder was directly used in transesterification reaction without calcination. Several experimental variables in the synthesis of calcium silicate mixed oxide

were considered to be critically affecting the catalytic capability: pH, CTAB amount and water amount. We also studied the variables in this order. Table 1 represents the summary of these prepared catalysts.

2.2.2 Development of Phosphoric Acid Monoester-Directed Mesoporous Calcium Silicate (PMCS) catalysts

In addition to optimizing the calcium silicate materials, we chose a phosphoric acid monoester (PME) surfactant, 3,6,9,12-tetraoxatricos-22-enyl dihydrogen phosphate, as the structure-directing agent for the synthesis of novel mesoporous calcium silicate materials. The anionic surfactant was synthesized according to the reported literature [3]. After obtaining the surfactant, we prepared another mixed oxide family by co-condensation reactions. Here, PME served as the surfactant (S^-) micelles templates, calcium (metal ion, M^+) ions and then hydrolyzed TEOS (inorganic precursor, I^-) coordinate accordingly, based upon electrostatic interactions, in the $S^-M^+I^-$ system [4, 5]. The PME surfactant in 100 mL of water was heated to 80 °C and then adjusted to pH 11.5. TEOS (1 mL) was introduced at once and solid calcium hydroxide was gradually added to the mixture. The reaction was carried out at 80 °C for 1 h under vigorous stirring, followed by aging at 90 °C for 24 h. The as-synthesized product was collected by hot filtration and washed with copious amount of water and methanol. Surfactant was removed by calcination at 600 °C for 6 h.

2.3 Transesterification of soybean oil and poultry fat into biodiesel

In order to correctly evaluate the catalytic ability of modified calcium silicate materials and to have direct comparison between catalysts, we followed the experiment procedures that were reported previously [2]. The procedures for the transesterification of soybean oil are: The mixture of 200 mg of dried solid catalyst and 24 mL of methanol was

stirred for 20 min to uniformly disperse the particle. Soybean oil (1.0 g) was then added into the mixture that prepared above. (All reactants are kept at the same mole ratio if not at the same amounts.) After 100 % conversion was reached, the mixture was filtered by a glass frit.

In the case of poultry fat, 35 mL of methanol was used along with 350 mg of the dried catalyst, and the resulting solution was stirred for 20 min at reflux condition to disperse the catalyst. Poultry fat (0.5 g) was then added into the catalyst solution that described above. After 100 % conversion was reached, the mixture was filtered by a glass frit.

In both cases, the filtrate was evaporated under vacuum to remove methanol and $CDCl_3$ was added for ^1H NMR analysis. Therefore, the conversion percentage of transesterification reaction can be obtained based upon the ratio of methyl protons (~3.6 ppm) to methylene hydrogens (α protons next to carbonyl group, 2.3 ppm).

2.4 Material Characterization and Analysis

Powder X-ray diffraction patterns were measured by Scintag Powder X-ray instrument. Micromeritics ASAP and Tristar apparatuses were used for nitrogen physisorption isotherms, BET, and BJH measurements. Chemisorption of materials was measured using Micromeritics AutoChem II. TEM electronmicrographs were obtained by using Tecnai G2 F20 Transmission Electron Microscope. Solid-state NMR was used to determine Ca/Si ratio of materials by ^{29}Si DPMAS and ^1H-^{29}Si CPMAS methods on a Varian-Chemagnetics Infinity 400 spectrometer.

Results and Discussions

3.1 Development and Catalysis of nonporous calcium silicate mixed oxide.

Mesoporous silica mixed oxide has been demonstrated to catalyze heterogeneous transesterification reaction [2]. In these experiments, calcium oxide, magnesium oxide, and barium oxide were added separately into the co-condensation reactions, and the mesoporous calcium silicate showed the best catalytic activity in biodiesel synthesis [2]. Nevertheless, the reaction kinetics of mesoporous calcium silicate, compared to that of homogeneous catalysts, is very slow. In this work, our primary goal is to develop heterogeneous catalysts for biodiesel synthesis with fast reaction kinetics.

In the synthesis of mesoporous materials, the pH of the solutions was usually highly basic or highly acidic to assist TEOS hydrolysis [6, 7]. The synthesis of mesoporous calcium silicate is a modification of MCM-41 [2, 6], which is under basic condition. Therefore, the first variable that we considered to be adjusted was pH. The pH of the solution affects not only the rate of hydrolysis of TEOS but the solubility of CaO in the synthesis of mesoporous calcium silicate catalysts. The result is shown in Figure 1. By lowering the solution pH from 12.3 to 9~10, the reaction kinetics of biodiesel conversion was improved by a factor of 2 (~12 h). As we continued to decrease the amount of NaOH added, the reaction time went up and became very long when the pH of the solution is weakly acidic.

The second parameter to be adjusted was the amount of CTAB. The role of CTAB in mesoporous material synthesis is to create templates which guide hydrolyzed silanes to form mesoporous structures [6, 7]. As a consequence, changing the CTAB amount could lead to change of pore formation, pore size, pore pattern, surface area, and possibly the catalytic activity of mesoporous calcium silicate material. The reduction or elimination of the usage of CTAB would offer economical and environmental benefits. Therefore, we tried to lower the amount of CTAB used in synthesis while monitoring the catalytic ability of the mixed

oxide. The result of this study is depicted in Figure 2. Upon lowering the CTAB amount from 1.0 g to 0.75 g, the reaction kinetics dropped a factor by 2. As we kept lowering the CTAB amount to 0.5, 0.4, and 0.3 g, the reaction rate remained almost constant, and its completion took 20~25 h. When CTAB was completely eliminated, the reaction kinetics was surprisingly fast and it took only 4.5 h to complete.

We also studied the possibility of reducing the consumption of water. However, the mixed oxides synthesized using less water exhibited lower catalytic activity in biodiesel production (Figure 3).

Our most active catalyst, CS-9, was prepared as following: we first mixed 480 mL water and 3.5 mL 2mM NaOH (pH 9.2), and heated the solution to 80 °C. 5 mL of TEOS was introduced at a rate of 30 mL/h by a syringe pump, and 0.5 g of CaO powder was added gradually three minutes after introducing TEOS. After the addition of TEOS and CaO was completed, the cloudy mixture was stirred at 80°C for 2 h, followed by hot filtration. The filter cake was washed by copious amount of water and then methanol. Since CTAB was used, calcination of the solid material was not necessary. The catalyst became ready to be used in biodiesel synthesis after drying in lyophilize.

Table 2 lists physical properties of the CS-9 and CS-1 catalysts. The surface area of CS-9 is 33 m^2/g, which is more than an order of magnitude below that of CS-1 catalyst or other mesoporous materials [2, 6, 7]. In order to explain the higher catalytic ability of CS-9, we point out that the mesoporous calcium silicate is synthesised under highly basic condition (pH = 12.2) and elevated temperature, which greatly affects the hydrolysis of TEOS and solubility of CaO. Under such conditions, TEOS hydrolysis and coordination of the negatively charged silane molecules with positively charged CTAB micelles take place very

rapidly. One the other hand, calcium oxide has to transform from solid to solvated CaO, before co-condensing with the silica matrix. Under high pH and temperature, not only the solubility of CaO is low but the solvation process is slow compared to the hydrolysis of TEOS. As a consequence, these two competing processes result in two phases. The majority of CS-1 surface (and other mesoporous calcium silicate catalysts) has the MCM-41-like mesoporous structure which contains very little calcium oxide. The rest of the material is amorphous, calcium-rich, and has low surface area. Consequently, the calcium domains are not readily accessible to fat molecules. In addition, the catalytic activity of mesoporous catalysts is restrained by the molecular diffusion. Triglyceride molecules are only slightly smaller that the pores of MCM-41 type materials, which restricts their ability to diffuse into the pore, reach the active catalytic site, react with methanol, and then diffuse out of the pore, if the active site is located deeply within the pore. Consequently, the large surface area associated with the mesoporous structure plays little role in the CS-catalyzed biodiesel synthesis. On the other hand, solid-state NMR measurements (see Table 2) indicated that the Ca/Si ratio in CS-9 (5.3) is much higher than in CS-1 (1.0), offering more catalytic sites and better reactivity. Other factors that may contribute to the observed difference in activity are still under investigation.

The TEM and SEM images of CS-9 show non-porous spherical nanoparticles (Figure 4, Table 2) of roughly 600 nm in diameter. The powder X-ray diffraction results (Figure 5) do not show peaks characteristic of crystalline CaO, which indicates that calcium oxide is incorporated into the matrix of the material. As highlighted in Table 2, the synthesis of CS-9 does not involve calcination and is carried out at half of the cost of the mesoporous catalyst.

In contrast to calcium oxide or homogeneous catalysts used in biodiesel synthesis [8, 9], the CS-9 catalyst is recyclable. In the case of SBO, as shown in Figure 6(a), the CS-9 has been recycled nine times with average loss of 4 percent of catalytic activity per cycle (figure 6a). The activity loss is attributed to the decrease in reduction in Ca/Si ratio, which dropped to 2.9 after 9 reactions, as shown by solid-state NMR. However, the reaction kinetics of CS-9 is still much faster than that of CS-1, even after recycling. In the case of poultry fat (Figure 6b), the CS-9 completed the reaction in 8.7 h (CS-1 took more than 48 h) and could be recycled 3 times without loss in reactivity.

3.2 Development and Catalysis of PMCS

Anionic surfactants have also been used as template agents to prepare mesoporous silica materials [3, 4, 10-14]. Here, positively charged calcium ions were added to interact with the phosphate groups of the surfactants. Under basic conditions, hydrolyzed TEOS easily coordinates with the calcium/surfactant in the $S^-M^+I^-$ complex system and forms ordered structure [3, 4]. After removing the surfactants, the calcium sites were exposed to the surface and therefore could react with methanol and feedstock easily. Table 3 represents the optimization processes of the PMCS catalysts. Initially, we synthesized materials using lower amounts of calcium hydroxide under various pH conditions, which resulted in poor catalytic activity during transesterification reaction (PMCS 1-3). However, the PMCS started to catalyze the transformation upon increasing the amount of $Ca(OH)_2$ gradually at pH of 11.5. As shown in Figure 7, when the amount of calcium hydroxide was increased to 74 mg (PMCS-4, see Table 3), the reaction was completed in 10 h. After doubling this amount, the reaction time was shortened to 2 h (PMCS-5). However, further increase of the

Ca(OH)$_2$ concentration during the synthesis slowed down the kinetics of biodiesel production dramatically. For example, the catalyst prepared using 296 mg of Ca(OH)$_2$ (PMCS-6) took more than 20 hours to complete the transformation. We found that the catalysts with optimum calcium content had almost identical reactivity when pH is in the range from 10.3 to 12.15 (PMCS 5, 8, 9), but lost it upon lowering the pH to 9 (PMCS-7). The PMCS catalysts could be reused 8 times without loss of reactivity after calcination at 600 ^{o}C for 6 h. However, the PMCS catalyst collected by direct filtration and lypholization after reaction did not yield good recyclability (~50% yield at 2 h for the second cycle). This could be due to the surface of catalysts being partially occupied by the reactant molecules, which is still under investigation.

Figure 8a shows the results of low angle powder X-Ray diffraction patterns of the PMCS materials. The catalyst with the lowest calcium loading (PMCS-3) exhibits d$_{100}$, d$_{200}$, and d$_{300}$ strong characteristic peaks of well-ordered lamellar structures, which is expected based on previous reports on the S$^-$M$^+$I$^-$ synthesis route [3, 4]. However, these patterns decrease with increasing calcium content and vanish completely in PMCS-6. The high angle diffraction patterns of PMCS-4, PMCS-5 and PMCS-6 catalysts (Figure 8b) exhibit peaks at 2θ $\cong$ 29~30° similar to those of active calcium silicate catalyst layers observed in mesoporous calcium silicates [2, 15]. Note that this peak is only present in catalysts which were active for biodiesel transformation. Besides, PMCS-3 and PMCS-4 exhibit a peak at 26°, attributed to the formation of hydroxyapatite, which is not catalytically acytive. At the same time, PMCS catalysts showed no presence of characteristic peaks from crystalline calcium oxide, indicating that calcium is incorporated into the matrix of the material. The nitrogen adsorption-desorption isotherm of PMCS-5 is shown in Figure 9. It presents a type

III mesostructure with type H3 hysteresis [16] and therefore confirms that it is a plate-like structure. The surface area of the PMCS-5 catalyst is 150 m^2/g.

3.3 Chemisoption Properties of CS-9 and PMCS-5 Catalysts

The chemisorption measurements are based on temperature-programmed-desorption (TPD) of pyridine adsorbed on catalysts (Table 4). The pyridine desorption on CS-9 and PMCS-5 occurred at 156.6 and 175.2 °C, respectively. The pyridine amounts obtained from TPD curve are 0.01 and 0.38 mmol/g for CS-9 and PMCS-5 while the reference material, 250 nm bare silica bead, showed no absorption of pyridine. This result suggested that these synthesized calcium silicate solid materials are slightly Lewis acidic and thus are able to catalyze free fatty acid to biodiesel [2].

Conclusions

Two new catalysts for biodiesel production have been developed, which are highly efficient, environmentally friendly, inexpensive, and easy to prepare. A non-porous calcium silicate mixed oxide catalyst for transesterification reactions, CS-9, improves the reaction kinetics by a factor of ~6. It can be recycled 9 times with an average activity loss in SBO of 4 percent, and 3 times without decrease in activity for PF. Its preparation requires no surfactants and therefore no calcination process is involved. PMCS-5, a lamellar catalyst prepared by phosphoric acid monoester surfactant, catalyzed the transformation in 2 h and can be reused 8 times after regeneration by calcination. This research exemplifies new opportunities for the development of greener technologies for generation of alternative fuels.

References

1. Ma F, Hanna M (1999) Biodiesel Production: a review. *Bioresource Technology* 70:1-15

2. Lin VSY, Nieweg JA, Verkade JG, Reddy Chinta RV, Kern C (2008) US Patent, Patent Publication Number US20080021232 A1

3. Pale-Grosdemange C, Simon ES, Prime KL, Whitesides GM (1991) J Am Chem Soc 113:12-20

4. Huo Q, Margolese DI, Ciesla U, Feng P, Gier TE, Sieger P, Leon R, Petroff PM, Schuth F, Stucky GD (1994) Nature 368:317-321

5. Che S, Garcia-Bennett AE, Yokoi T, Sakamoto K, Kunieda H, Terasaki O, Tatsumi T (2003) Nat Mater 2:801-805

6. Kresge CT, Leonowicz ME, Roth WJ, Vartuli JC, Beck JS (1992) Nature 359:710-712

7. Zhao D, Feng J, Huo Q, Melosh N, Frederickson GH, Chmelka BF, Stucky GD (1998) Science 279:548-552

8. Venkat Reddy CR, Oshel R, Verkade JG (2006) Energ Fuel 20:1310-1314

9. Kouzu M, Yamanaka SY, Hidaka JS, Tsunomori M (2009) Appl Catal A-Gen 355:94-99

10. Garcia-Bennett AE, Kupferschmidt N, Sakamoto Y, Che S, Terasaki O (2005) Angew Chem Int Ed 44:5317-5322

11. Garcia-Bennett AE, Miyasaka K, Terasaki O, Che S (2004) Chem Mater 16:3597-3605

12. Gao C, Sakamoto Y, Sakamoto K, Terasaki O, Che S (2006) Angew Chem Int Ed 45:4295-4298

22

13.   Gao C, Qiu H, Zeng W, Sakamoto Y, Terasaki O, Sakamoto K, Chen Q, Che S (2006) Chem Mater 18:3904-3914

14.   Gao C, Sakamoto Y, Terasaki O, Che S (2008) Chem Eur J 14:11423-11428

15.   Chen JJ, Thomas JJ, Taylor HFW, Jennings HM (2004) Cement Concrete Res 34:1499-1519

16.   Kruk M, Jaroniec M (2001) Chem Mater 13:3169-3183

Figures and Tables

Sample Code	CTAB (g)	TEOS (mL)	CaO (g)	pH* value	H$_2$O (mL)
CS-1	1	5	0.5	12.2	480
CS-2	1	5	0.5	10.2	480
CS-3	1	5	0.5	9.2	480
CS-4	1	5	0.5	6.0	480
CS-5	0.75	5	0.5	9.2	480
CS-6	0.5	5	0.5	9.2	480
CS-7	0.4	5	0.5	9.2	480
CS-8	0.3	5	0.5	9.2	480
CS-9	0	5	0.5	9.2	480
CS-10	0	5	0.5	9.2	250
CS-11	0	5	0.5	9.2	100

Table 1. Preparation of Mixed Oxide Materials by Modified Calcium Silicate Method

*The pH values were measured at 25 °C before the introduction of CaO. For pH below 7, HCl was used.

Properties	CS-9	CS-1
Time for 100 % yield* (hr)	4.5	30
Surface area (BET) (m^2/g)	33	443
Pore size (BJH) (nm)	Non-porous	< 2
Ca/Si ratio from solid-state NMR	5.3	1.7
Structure	Solid sphere	Mesoporous
Estimated cost of preparation	50%	100%
Calcination condition	none	600 °C for 6 hrs

Table 2. Comparison of CS-9 and CS-1. *Feedstock: SBO

Entry No	PME (mg)	$Ca(OH)_2$ (mg)	TEOS (mL)	H_2O (mL)	pH* value
PMCS-1	185	37	1	100	3.4
PMCS-2	185	37	1	100	9.0
PMCS-3	185	37	1	100	11.5
PMCS-4	185	74	1	100	11.5
PMCS-5	185	148	1	100	11.5
PMCS-6	185	296	1	100	11.5
PMCS-7	185	148	1	100	9.0
PMCS-8	185	148	1	100	10.3
PMCS-9	185	148	1	100	12.2

Table 3. Synthesized PMCS Catalysts by the Phosphate Monoester Surfactant.

Material	Pyridine absorbed (mmol/g)	Peak temp (°C)	Surface area (m^2/g)
Silica nanoparticles*	No peak	NA	10
CS-9	0.01021	156.6	33
PMCS-5	0.38501	175.2	150

Table 4. Chemisorption Results of Absorbed Pyridine by Catalysts

* 250 nm, synthesized by Stober method

** Pyridine absorption at 120 °C. TPD program: 10 °C/min heating ramp from 120 to 600 °C, total duration for TPD is 2 h.
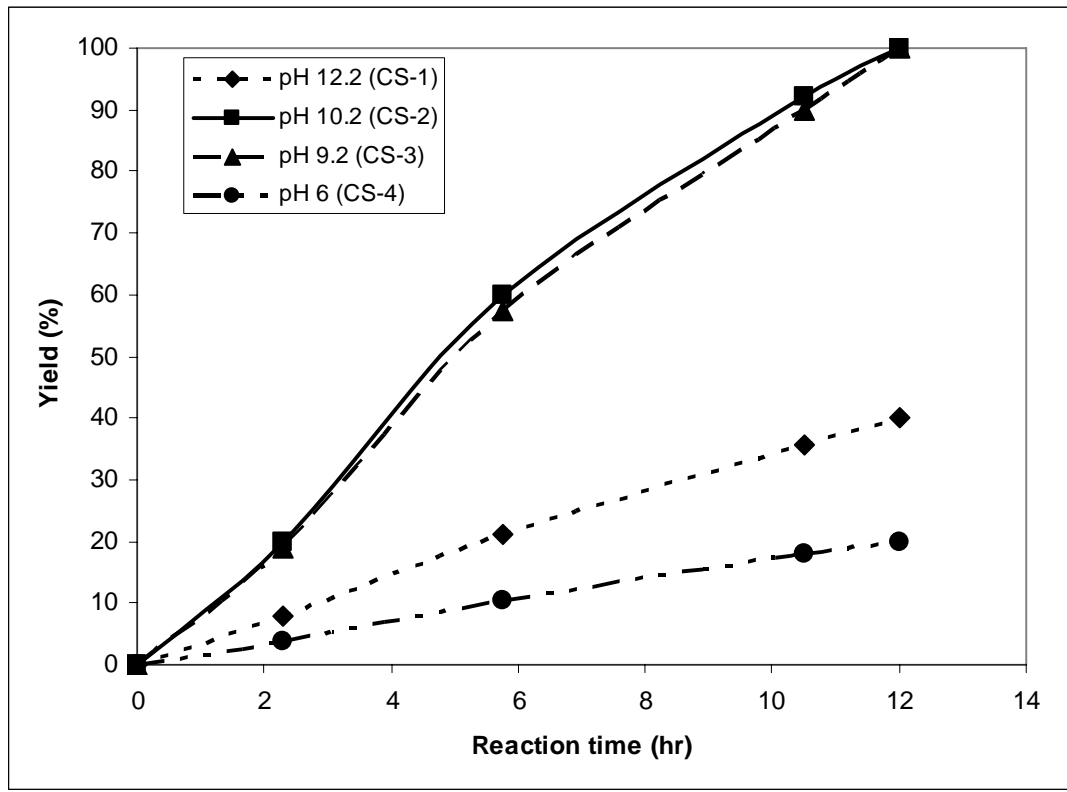
Figure 1. Comparison of catalytic ability of different calcium silicate materials: the pH study. The catalytic activity of MCS materials is strongly influenced by the solution pH during the synthesis of catalysts. Numbers in parenthesis
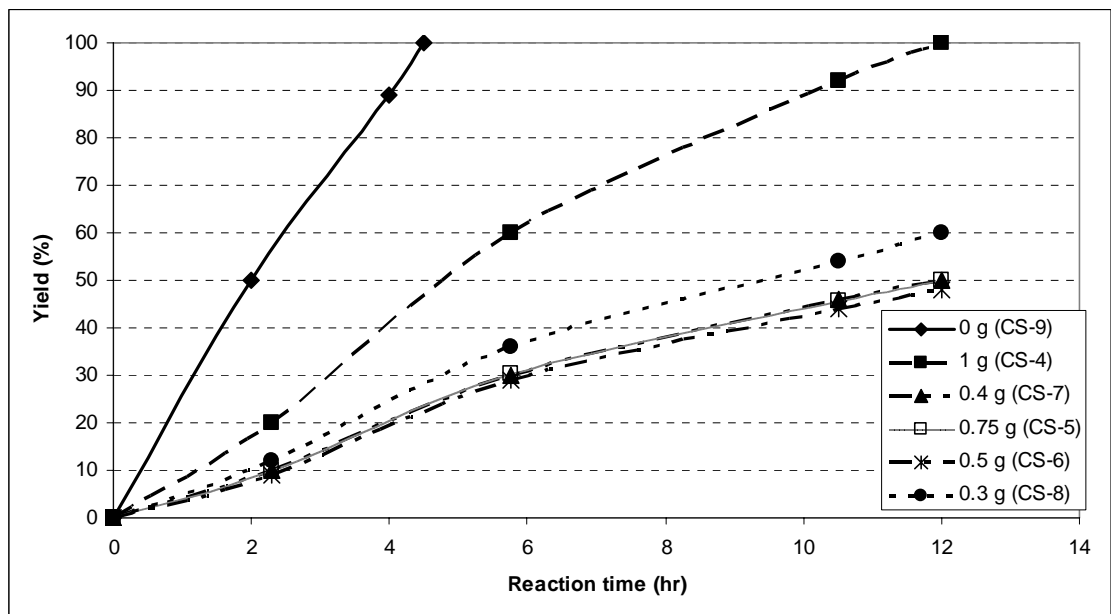
Figure 2. Comparison of the catalytic performance of different materials as a function of

CTAB concentration.
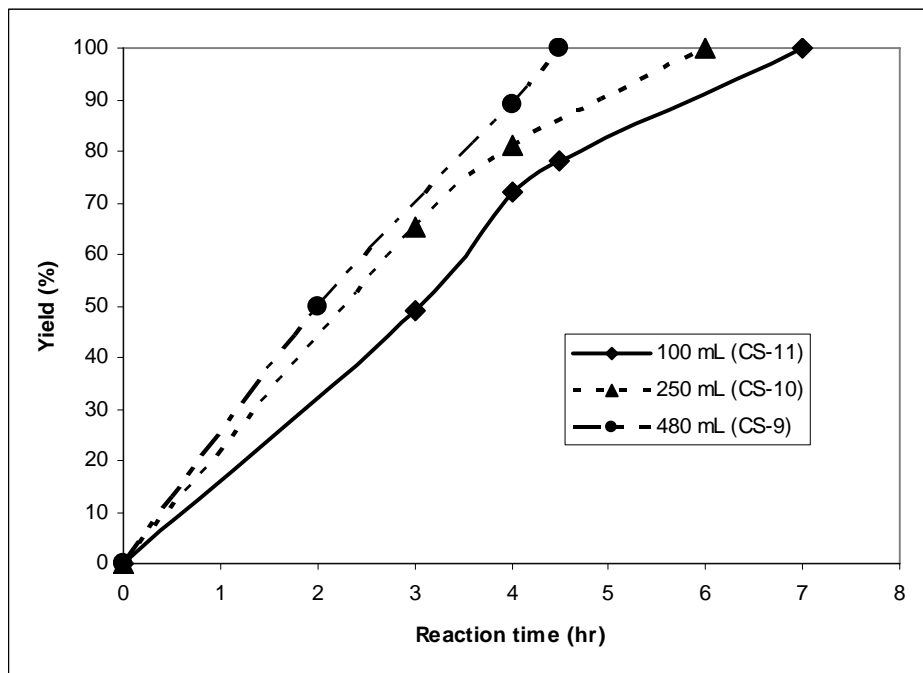
Figure 3.   Comparison of the catalytic performance of different materials as a function of amount of water used during the synthesis.
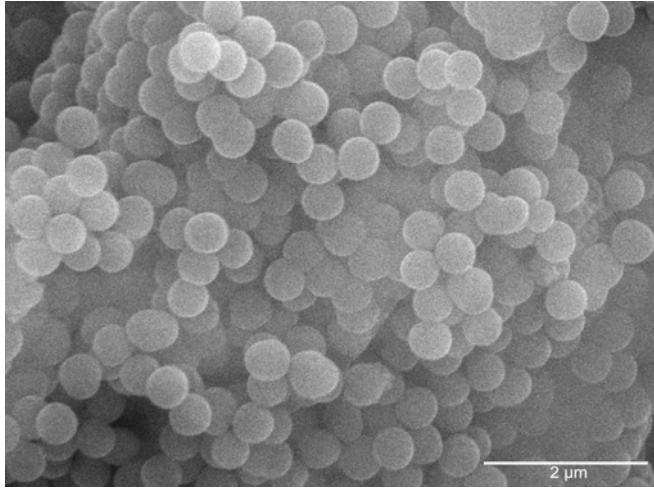
(a) SEM image
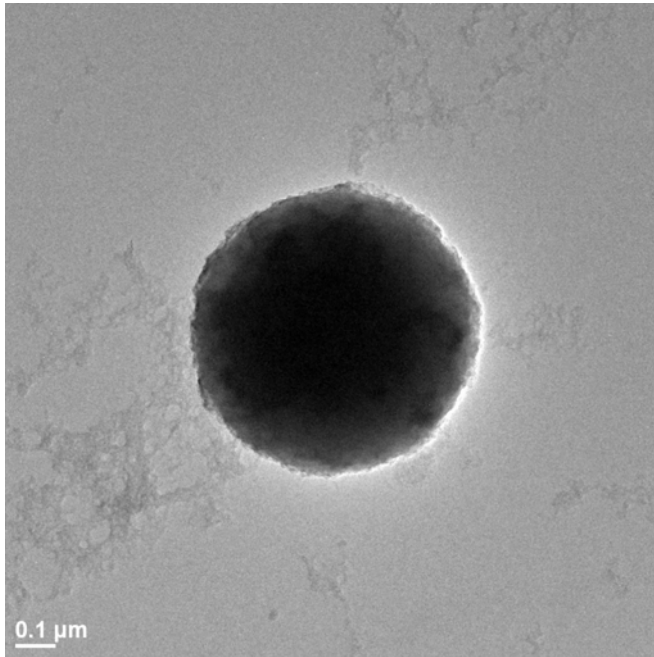
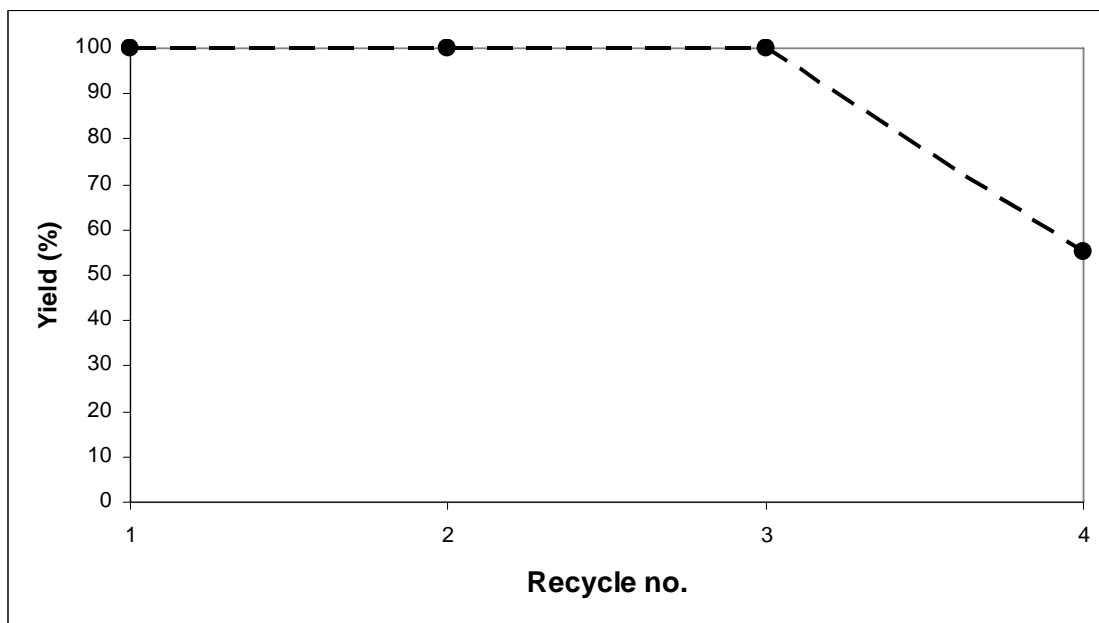(b)TEM image

Figure 4. SEM (a) and TEM (b) images of CS-9.
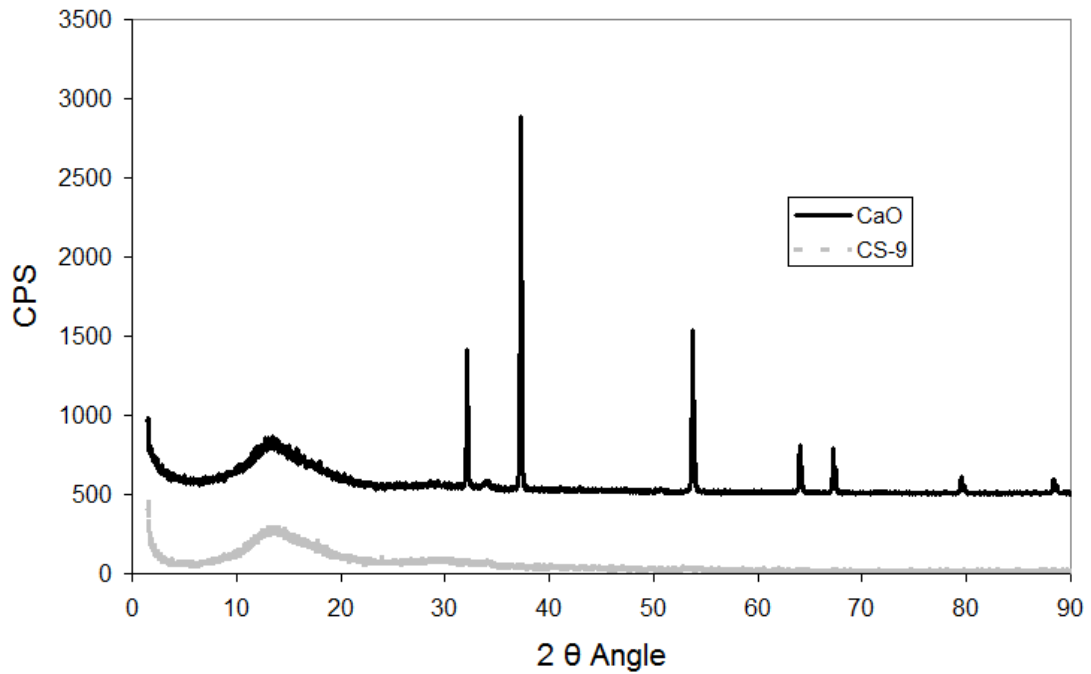
Figure 5. Powder X-ray diffraction results of CS-9 and CaO.
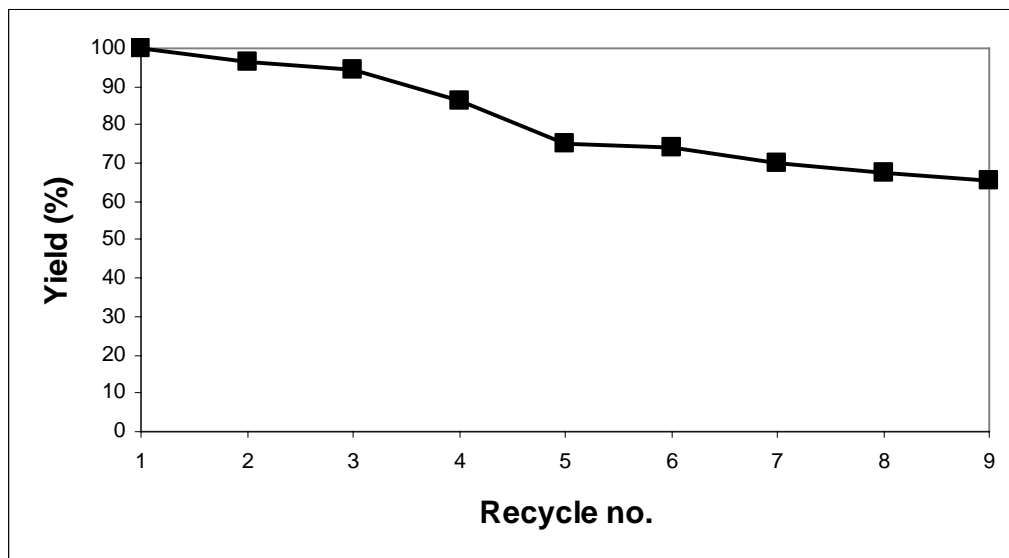
(a)

(b)

Figure 6. Recyclability of CS-9 in (a) SBO and (b) PF. For SBO, the yield was

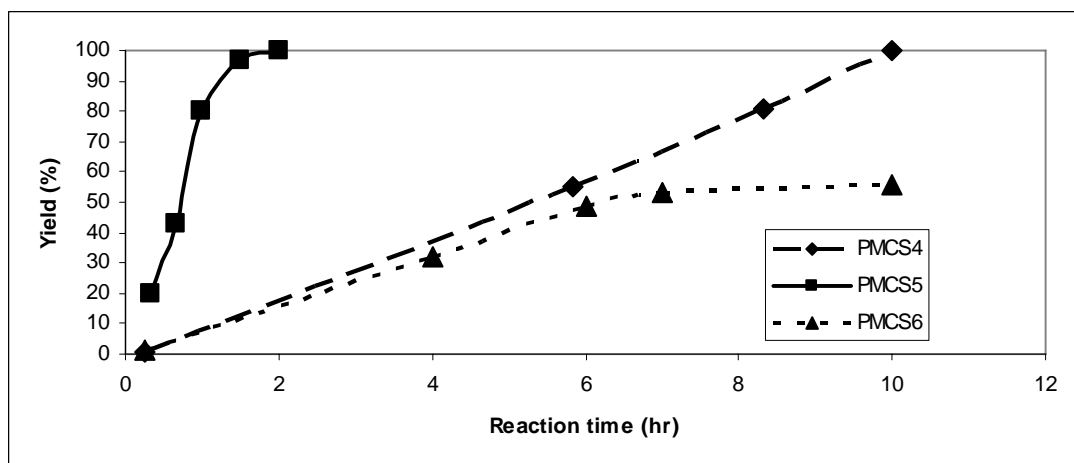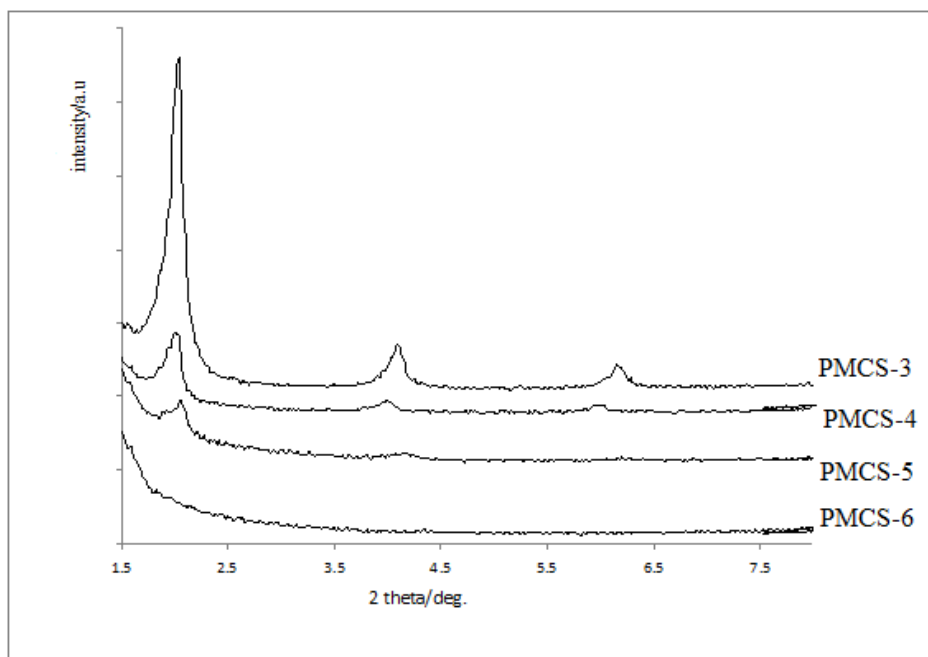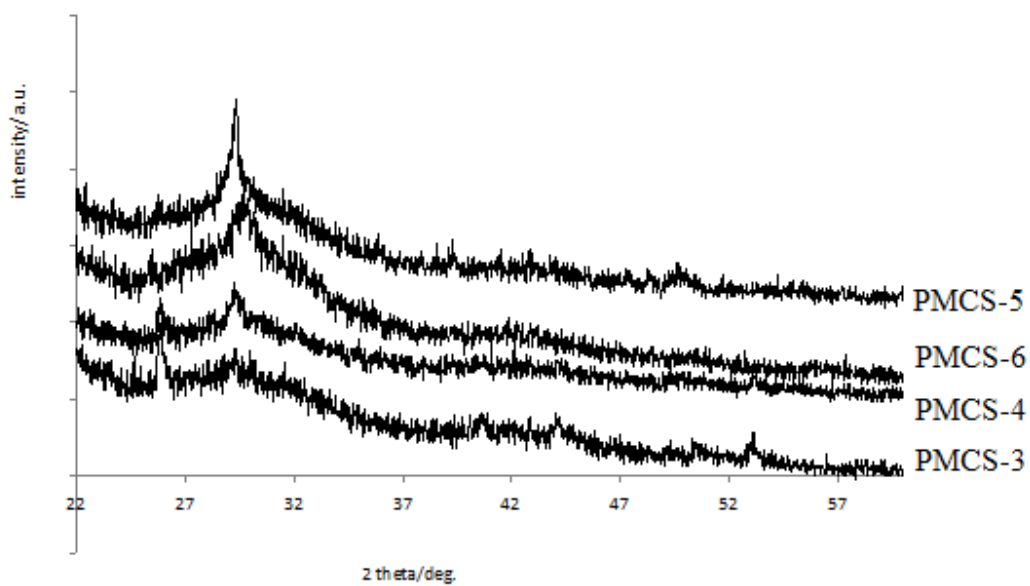determined at 4.5 h; for PF the yield was determined at 8.7 h.

Figure 7. Optimization of calcium oxide concentration in PMCS catalysts.

(a) Low angle

(b) High angle

Figure 8. Powder X-ray patterns of PMCS catalysts at (a) low and (b) high angle.
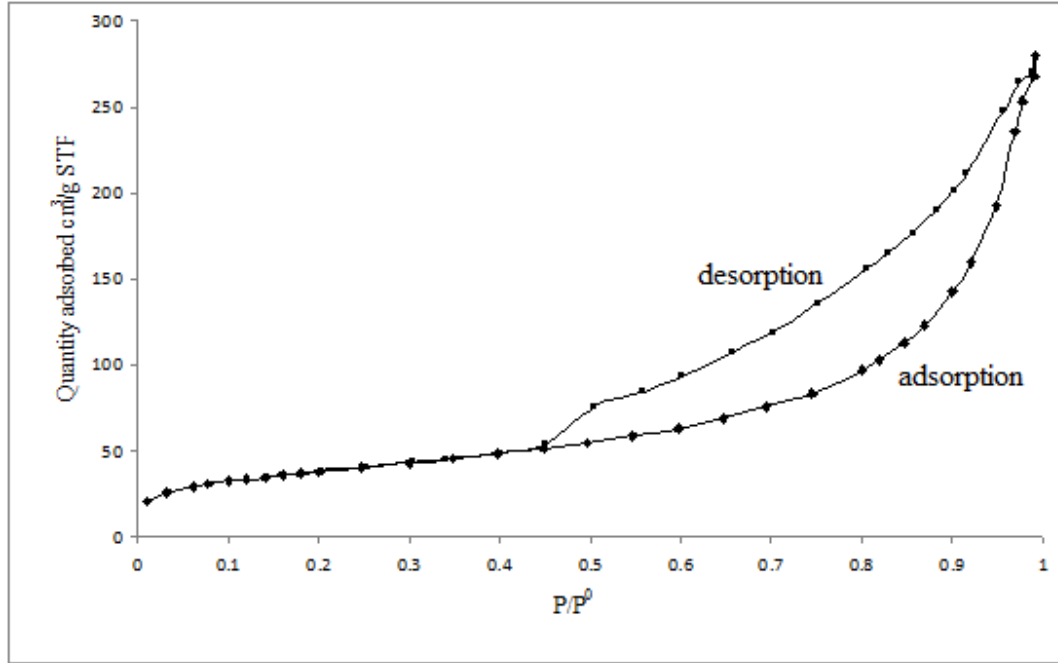
Figure 9. Nitrogen adsoption-desorption isotherm of PMCS-5

CHAPTER 3 RH-BASED MESOPOROUS MANGANESE OXIDES FOR SELECTIVE SYNTHESIS OF ETHANOL FROM SYNGAS

Abstract

In this study, mesoporous manganese oxides were successfully synthesized. 2%Rh was loaded to the mesoporous manganese oxides and its catalytic performance was tested. The Rh/Mn oxides show better selectivity and reactivity than the Rh-Mn/SiO$_2$. The temperature studies show that the reactivity of the Rh/Mn oxides increases by 10% per 10°C. The selectivity towards ethanol remains approximately the same when the temperature increases from 280°C to 310°C and decreases after 310°C. This may due to the structure change of the mesoprous manganese oxides and the agglomeration of the Rh particles.

Introduction

Ever since the oil crisis, people have been searching for alternative energy sources. Biomass becomes an important candidate because it is renewable, biodegradable and nontoxic. Biomass can be converted into a wide range of biofuels, such as bioethanol and biodiesel. Among those biofuels, bioethanol can be additive and potential substitute for gasoline, as well as a feedstock for synthesis of a variety of chemicals. As a result, ethanol receives more and more attentions. There are several ways to produce bioethanol, such as fermentation of sugar, hydrogenation of petroleum-based ethylene and synthesis from syngas.[1]Syngas is a gas mixture that contains primarily of carbon monoxide and hydrogen. It is obtained by gasification of biomass, coal, and petroleum coke and residue.

The heterogeneous catalysts used for converting syngas to alcohol can be broadly classified into four categories, Rh-based, modified Mo-based, modified Fischer-Tropsch type and modified methanol synthesis catalysts.[1, 2] Rh is most often used as a catalyst for producing C_2^+ oxygenates, i.e. ethanol, acetaldehyde and acetic acid, from syngas. It is because Rh lies among metals such as Fe and Co which can easily dissociate CO to form higher hydrocarbons, and Pd, Pt and Ir which do not dissociate CO and produce methanol.[1-5] It is reported that it can increase the ethanol selectivity through adding promoter, such as Mn,[6] Fe[7] and V. In order to find the effective and selective catalysts, numerical researches have been devoted to study the reaction and mechanism of formation of C_2^+ oxygenation on the Rh-Based catalysts. Those studies mostly employ IR，CO-TPD, TPR, TPSR and XPS techniques. It is commonly recognized that the formation of C2 oxygenations over Rh-based catalysts requires absorption and dissociation of H_2 and CO, hydrogenation of CH_x, CO insertion to alkyl bond and followed by further hydrogenation. The adsorption of CO on the catalyst surface is important and it is affected by the prompters, supporters, Rh cluster size and reaction conditions.[1] There are tilted, linear, geminal and bridged forms of CO absorbed on the catalytic surfaces. Bao and his co-worker proposed that among these four forms of CO species, the tilted one, which was the main precursor for dissociation, could lead to ethanol formation, and that addition of promoter could increase the amount of CO with tilted form.[8] He also pointed out that the catalytically active site was $(Rh^0Rh^+)-O-M^{n+}$, where located the promotor M^{n+} to help create a new active site for CO insertion. In addition, the $O-M^{n+}$ bonds could also help the CO dissociation. The detailed mechanism is shown in Figure 1.Besides the promoter effects, the supporter also plays an important role. As a result, many researchers

used high surface area supporter, such as mesoporous SiO_2 and Al_2O_3 as supporter to increase the dispersion of Rh.

Mn is quite often used to promote Rh recently. Ojeda[9] studied the Mn loading effects by preparing four Rh-Mn/Al_2O_3 catalysts with different Mn/Rh ratios. He found that reactivity increased as the Mn/Rh ratio increased because more and more Rh clusters had close interaction with Mn which leads to higher catalytic activity per Rh atom, although the Rh maybe partially block by Mn. The selectivity towards oxygenations reached a maximum when Mn/Rh ratio is one. when the Mn/Rh ratio was larger than one, the selectivity decreased as the Mn/Rh ration increased because the Mn decreased the relative Rh surface accessible to CO. In order to promote as many as Rh clusters and yet not to block the Rh surface, we designed mesoporous manganese oxide to support and also to promote Rh catalyst. It was found that the supporter, with high BET surface area up to 200m^2/g, not only increased the dispersion of Rh cluster, but also improved the promotion effect by creating more interaction between Rh and Mn.

In this work, Rh/Mn oxides were used to synthesis C2 oxygenations from syngas in a micro-tubular reactor. It is found that this catalyst can improve the selectivity and reactivity comparing to Rh-Mn/SiO2. Further more, the effect of temperature was also studied and 310°C is found to be the best temperature in terms of highest ethanol selectivity.

Experimental

1.Synthesis of mesoporous manganese oxides and 2%Rh/Mn oxides

4gMnNO$_3$ and 1.28gSDS were dissolved in 40mlH$_2$O. 1.28g H$_2$C$_2$O$_4$ and 0.75ml H$_3$PO$_4$ in 10mlH$_2$O was added slowly into the Mn^{2+} solution. After stirring over night, the white solid was collected and washed by water and methanol several times，followed by calcification at 450°C for 6hr with temperature ramp at 1°C/min. BET surface was measured to be around 200cm^2/g, and the pore size was 1~2nm. 2wt% of RhCl$_3$ was impregnated to mesoporous manganese oxides by conventional impregnations.

2.Synthesis of ethanol and C2 oxygenations from syngas on micro-tubular reactor

The micro-tubullar reactor, as shown in Figure 2, was equipped with a Parr temperature controller (Model4843, Parr Instrument Company, Moline, Illinois) with two type-K thermocouples and Parr mass flow system with Brooks mass flow controllers. 0.3g catalyst and 3g catalyst diluting reagent SiC were loaded into the reactor. The catalyst was purged with Ar (20mL/min) for 30min before reduced by hydrogen (10 ml/min) at 300°C under 450 psi for 2 hours. Then the system was purged by syngas (H$_2$ / CO =2) for 15min before syngas was charged into the system until pressure was up to 450psi. The reaction was conducted at 300°C under 450psi with CO flow rate at 11mL/min and H$_2$ flow rate at 22mL/min. Deionized water was added to the condenser to dissolve the alcohol productions. The GC, (Varian 3900 with CP-Molsieve 5A (10m×0.32mm×10μm) and CP-PoraBOND Q (50m×0.53mm×10μm)) with a thermal conductivity detector with 5wt% Ar as internal standard, was use to analyse the tail gas every certain time, from which we can calculate CO conversion and gas product (such as methane, CO$_2$, ethane) selectivity. After reaction, liquid sample was collected from condenser and added with 1-butanol as internal standard. The mixture was analyzed using a Varian 3900GC with flame ionization detector and a CP-

PoraBOND Q (50m×0.53mm×10µm). From the GC result, we can find the liquid product concentration and selectivity as well.

Results and Discussion

Figure 3 shows the TEM of the mesoporous manganese oxides. The pore structure can be clearly seen and the pore size distribution is around 1~2 nm. Figures show the XRD of the Rh/Mn oxides after the reactions, which reveals that Mn has +2 oxidation state.

As shown in Table 1, the Mn promoted 2%Rh/SiO$_2$ shows better catalytic performance than the unprompted Rh/SiO$_2$, which is confirmed by previous literature. And the Rh/ Mn oxides have better catalyst activity than Rh-Mn/ SiO$_2$ synthesized by co-impregnation. One possible reason is that the Rh particles might be partial covered by Mn promoter, which makes the surfaceof Rh less accessible to CO and H$_2$. The other reason might be the better close interaction between Rh paticles and Mn in the Rh, which leads to higher catalyst reactivity. The Rh/ Mn oxides have higher selectivity towards ethanol than Rh-Mn/SiO2. It is because that some Rh particles in the Rh-Mn/SiO$_2$ might not be in close interaction with Mn and thus is unprompted. On the other hand, this also shows that the Mn can better promote Rh in the Rh/Mn oxides than the Rh-Mn/SiO$_2$.

Table 2 shows the temperature study which is conducted by choosing five different temperatures to study the effect of temperature on 2%Rh/Mn oxides. The CO conversion increases by approximately 10% as the temperature increases by 10$^{\text{o}}$C. The methane is thermodynamic favored product, thus the methane selectivity increases as the temperature increases. Since the methanol formation is not favored at high temperature, the methanol

selectivity is found to continuously decrease as the temperature increases. Ethanol formation is also unfavored at high temperatures based on the thermodynamic calculations[2]. But the selectivity towards ethanol keeps approximately the same when the temperature changes from 280°C to 310°C. It might be possible that at higher temperature, the Mn promotes the Rh particles better. When the temperature goes up to 320°C, there is a sudden drop of ethanol selectivity. The Mn oxides promoting effect is dropping at that temperature, which might be because of Rh aggregation or the structure changes of the mesoporous manganese oxides. Base on the thermodynamic and kinetic considerations, 310°C is the best reaction temperature for Rh/Mn oxides.

References

1.   Spivey, J. J.; Egbebi, A., *Chemical Society Reviews* **2007,** 36, (9), 1514-1528.

2.   Subramani, V.; Gangwal, S. K., *Energy & Fuels* **2008,** 22, (2), 814-839.

3.   Bhasin, M. M.; Bartley, W. J.; Ellgen, P. C.; Wilson, T. P., *Journal of Catalysis* **1978,** 54, (2), 120-128.

4.   Forzatti, P.; Tronconi, E.; Pasquon, I., *Catalysis Reviews-Science and Engineering* **1991,** 33, (1-2), 109-168.

5.   Poutsma, M. L.; Elek, L. F.; Ibarbia, P. A.; Risch, A. P.; Rabo, J. A., *Journal of Catalysis* **1978,** 52, (1), 157-168.

6.   Hu, J. L.; Wang, Y.; Cao, C. S.; Elliott, D. C.; Stevens, D. J.; White, J. F. In *Conversion of biomass-derived syngas to alcohols and C-2 oxygenates using supported Rh catalysts in a microchannel reactor*, 19th Meeting of the North-American-Catalysis-Society

41

(NAM), Philadelphia, PA, May 22-27, 2005; Elsevier Science Bv: Philadelphia, PA, 2005; pp 90-95.

7. Burch, R.; Hayes, M. J., *Journal of Catalysis* **1997,** 165, (2), 249-261.

8. Wang, Y.; Luo, H. Y.; Liang, D. B.; Bao, X. H., *Journal of Catalysis* **2000,** 196, (1), 46-55.

9. Ojeda, M.; Granados, M. L.; Rojas, S.; Terreros, P.; Garcia-Garcia, F. J.; Fierro, J. L. G., *Applied Catalysis a-General* **2004,** 261, (1), 47-55.
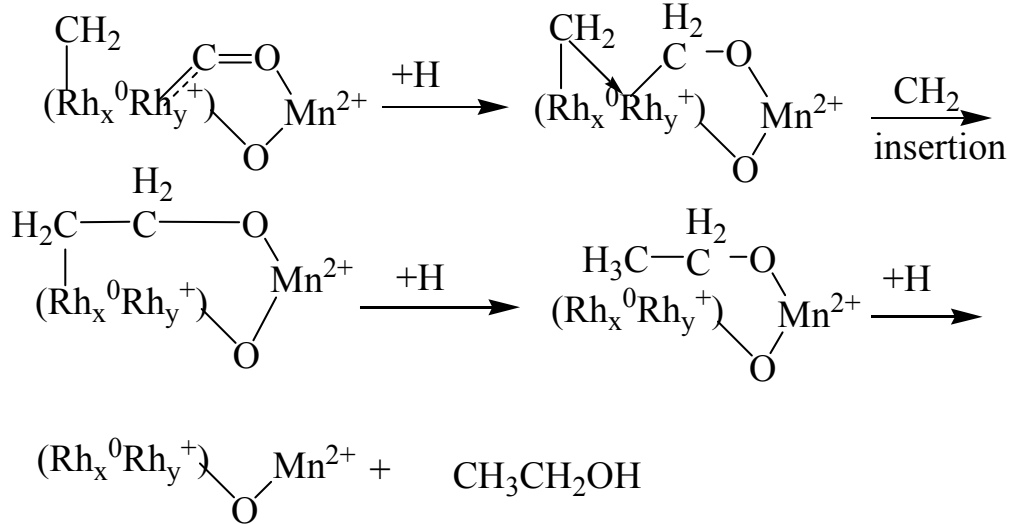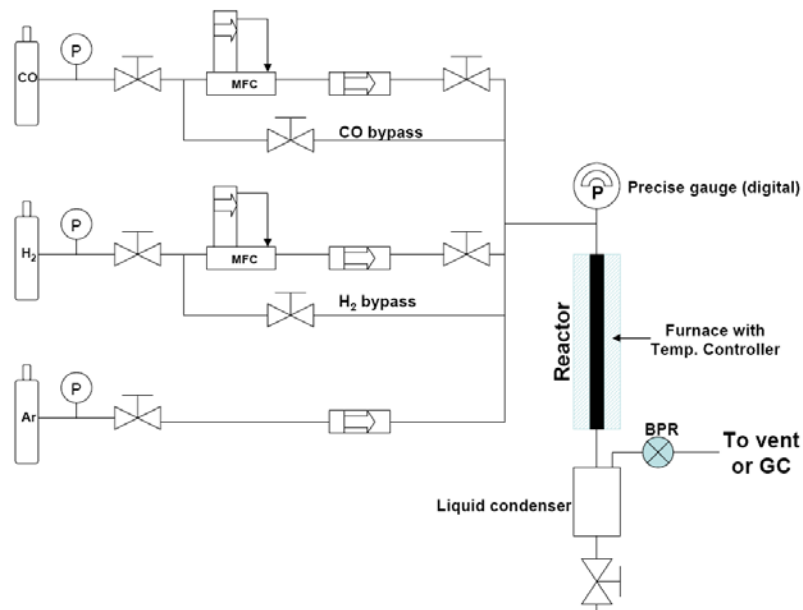
Figures and Tables

Figure 1 the mechanism of Ethanol formation on Rh-Mn/SiO$_2$ catalyst[6]
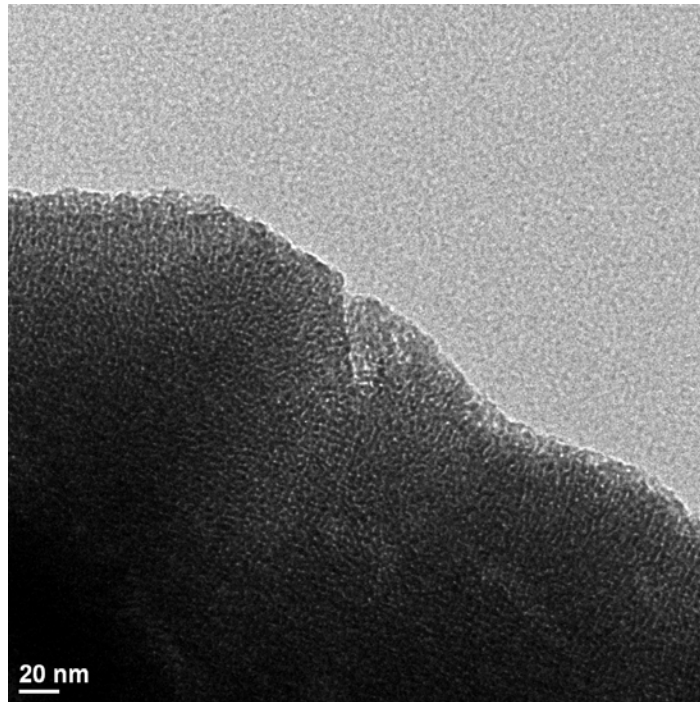

Figure 2 Scheme of a micro-tublar reactor
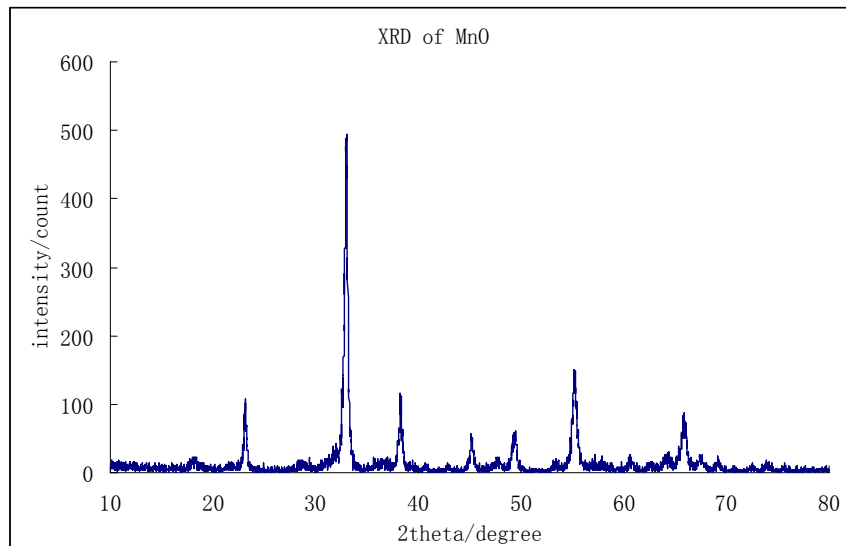
Fuigure 3.TEM image of mesoporous Manganese oxides

Figure 4. X-ray pattern of MnO

catalyst	experimental conditions				X_{CO}(%)	Carbon selectivity(%)				
	Temp (^{o}C)	Press (psig)	GHSV (mL·g^{-1}·h^{-1})	H_2/CO		H_4	CO_2	C_1-OH	C_2-OH	C2 oxygenations
2%Rh/SiO$_2$	300	450	6600	2	2.7	2.8	0	6.7	17.7	20.5
2%Rh-Mn/SiO$_2$ (Rh/Mn 1:1)	300	450	6600	2	13.7	2.7	1.6	3.8	22.9	24.3
2%Rh/MnO$_2$	300	450	6600	2	25.5	2	4.3	3.5	32	35.7

Table 1.Catalytic performances of 2%Rh/SiO$_2$, 2%Rh-Mn/SiO$_2$ (Rh/Mn 1:1) and

2%Rh/Mn oxides

catalyst	experimental conditions				X_{CO}(%)	Carbon selectivity (%)				
	temp (^{o}C)	Press (psig)	GHSV (mL·g^{-1}·h^{-1})	H_2/CO		H_4	CO_2	C_1-OH	C_2-OH	C2 oxygenations
2%Rh/Mn oxides	280	350	6600	2	5.4	3.4	2.3	6.8	33	41.9
2%Rh/Mn oxides	290	450	6600	2	12.1	5.3	2.7	3.3	33	37.2
2%Rh/Mn oxides	300	450	6600	2	25.5	2.0	4.3	3.5	32	38.6
2%Rh/Mn oxides	310	450	6600	2	38.9	2.2	4.9	2.5	33	40.4
2%Rh/Mn oxides	320	450	6600	2	47.6	2.5	5.3	1.4	18	27.8

Table 2.Temperature studies of the Rh/Mn oxides

CHAPTER 4. THE NMR MEASUREMENT OF CA/SI RATIO IN MCS AND THE CONCENTRATION OF FITC IN MSN

Part 1: Measurement of the Ca/Si ratio in MCS

NMR experiment

The ^{29}Si NMR spectra were obtained at 9.4 T on a Chemagnetics Infinity spectrometer using a 3.2-mm triple resonance probe. The ^{1}H-^{29}Si cross polarization (CP) and direct polarization (DP) methods were used for excitation, under magic angle spinning (MAS) at 10 kHz. The magnitudes of RF magnetic fields at the ^{1}H and ^{29}Si frequencies during CP were ν_{RF}^{H} = 65 kHz and ν_{RF}^{Si} = 55 kHz, respectively. Each CPMAS spectrum resulted from 5 K scans and was acquired in approximately 1 hour. The ^{29}Si DPMAS measurements involved 280 scans, a pulse delay of 300 s and total acquisition time of approximately 24 hours. The samples were packed into the MAS rotor, dried under 90^{0}C for 4hr and weighted.

Solid-State NMR Results

The Ca/Si ratios were estimated using two different methods. First, the ^{29}Si CPMAS spectra were deconvoluted into peaks representing separate Q^{n} groups to find the exact lineshape parameters. These parameters were used to deconvolute the ^{29}Si DPMAS spectra, which were quantitative but less intense. The Ca/Si ratios were then calculated in similar manner as the Si/Al ratio in zeolites. The same ratios were also measured using ^{29}Si spin counting, by comparing the total integrated intensity of Q^{n} groups in ^{29}Si DPMAS spectra of MCS materials with that of a reference sample of MCM-41. Both methods yielded similar results.

The NMR data show that the Ca/Si ratio decreased after several cycles of transesterification. The recyclability tests for both MCSH$_2$O and MCSethanol show loss of reactivity as illustrated in Figure1. These results suggest that the Ca/Si ratio plays an important role in the reactivity of MCS materials.[1]

Part 2: Measurement of the concentrations of FITC on MSN

NMR experiment

The ^{29}Si NMR spectra were obtained at 9.4 T on a Chemagnetics Infinity spectrometer using a 5-mm triple resonance MAS probe. The ^{1}H-^{29}Si CPMAS method was used for excitation, using MAS at 8 kHz, ν_{RF}^{H} during CP = 54 kHz, ν_{RF}^{H} during TPPM decoupling = 30 kHz, and ν_{RF}^{Si} during CP = 62 kHz. Each spectrum resulted from 32 K scans and was acquired in approximately 18 hours. The samples were packed into the MAS rotor as received, without any further treatment.

Short summary of the NMR results

Due to the very low concentration of T sites, the analysis of their concentration was carried out by ^{1}H-^{29}Si CPMAS experiment, instead of the time consuming DPMAS method.[2] The CPMAS spectra (shown in Figure 4) are not strictly quantitative, because the ^{1}H-^{29}Si CP process favors the sites that are in closer proximity to hydrogen. According to our previous report, the relative contribution of T sites to the CPMAS spectra is approximately 1.5 to 2 times higher than that measured by DPMAS.[3] By using a factor of 1.75 to scale down the

intensities observed in the CPMAS spectra, the amount of T sites was estimated at 0.65 ±0.11% in AEP, 0.52 ±0.08% in AL, 0.52 ±0.09% in AP and 0.62 ±0.11% in ICP. We conclude that within the error of our experiments the relative populations of T sites, and thus the concentrations of FITC are the same in all four MSNs.

Reference

1. Nieweg, J. A.; Kern, C.; Trewyn, B. G.; Wiench, J. W.; Pruski, M.; Lin, V. S. Y. In *Calcium oxide-porous silica catalyzed transesterification of biomass feedstocks*, 231st National Meeting of the American-Chemical-Society, Atlanta, GA, Mar 26-30, 2006; Amer Chemical Soc: Atlanta, GA, 2006; pp 819-INOR.

2. Trebosc, J.; Wiench, J. W.; Huh, S.; Lin, V. S. Y.; Pruski, M., Studies of organically functionalized mesoporous silicas using heteronuclear solid-state correlation NMR spectroscopy under fast magic angle spinning. *Journal of the American Chemical Society* **2005,** 127, (20), 7587-7593.

3. Wiench, J. W.; Lin, V. S. Y.; Pruski, M., Si-29 NMR in solid-state with CPMG acquisition under MAS. *Journal of Magnetic Resonance* **2008,** 193, (2), 233-242.

Figures and Tables

Sample	MCSH$_2$O	MCSH$_2$Oafter 9 cycles	MCSEthanol	MCSEthanol after 5 cycles
Ca/Si ratio	5.29	2.9	2.26	0.89

Table1. Ca/Si ratio of MCSH$_2$O and MCSEthanol calculated from spin counting
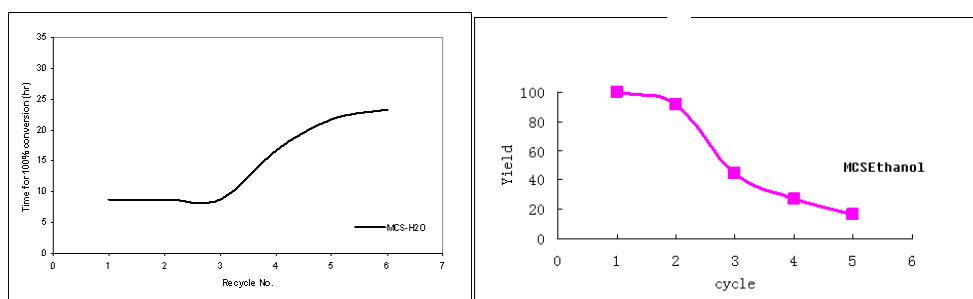
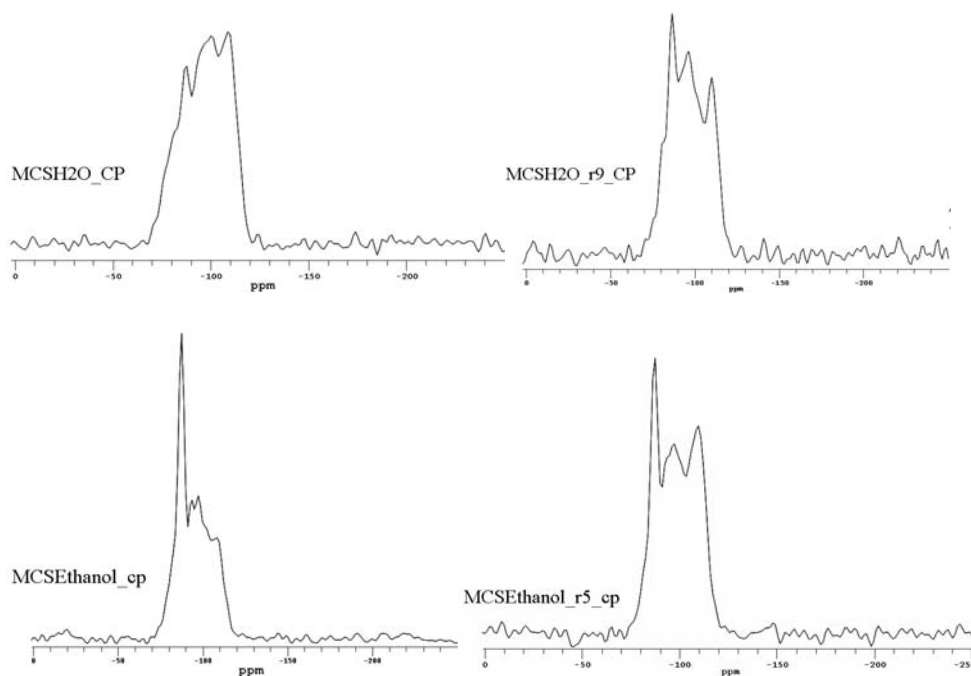**Figure1**.Recyclability of MCSH$_2$O and MCSEthanol with soybean oil as feedstock

Figure2. ^{1}H-^{29}Si CPMAS spectra of MCS
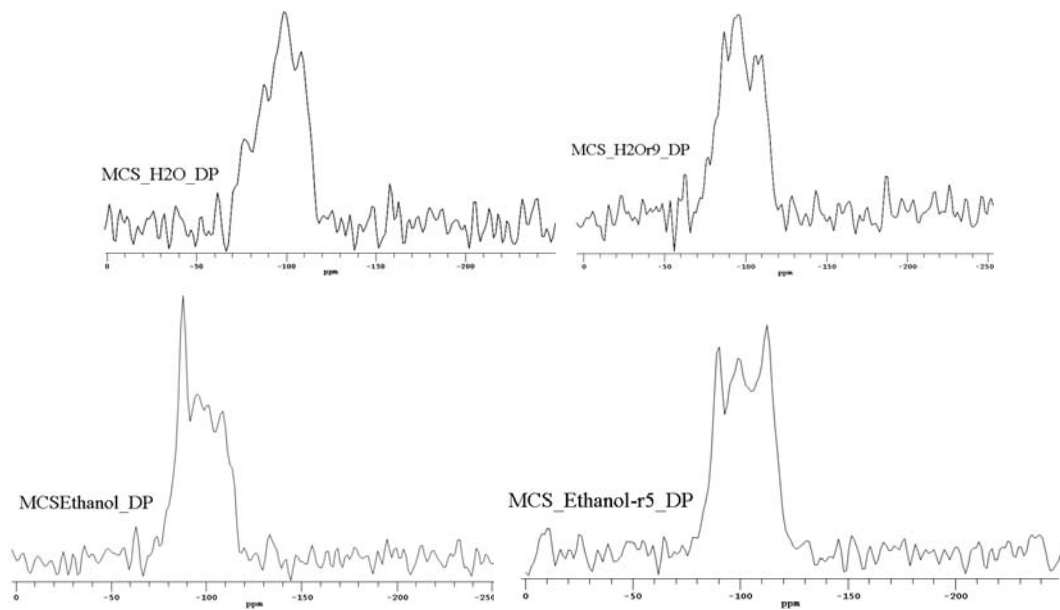
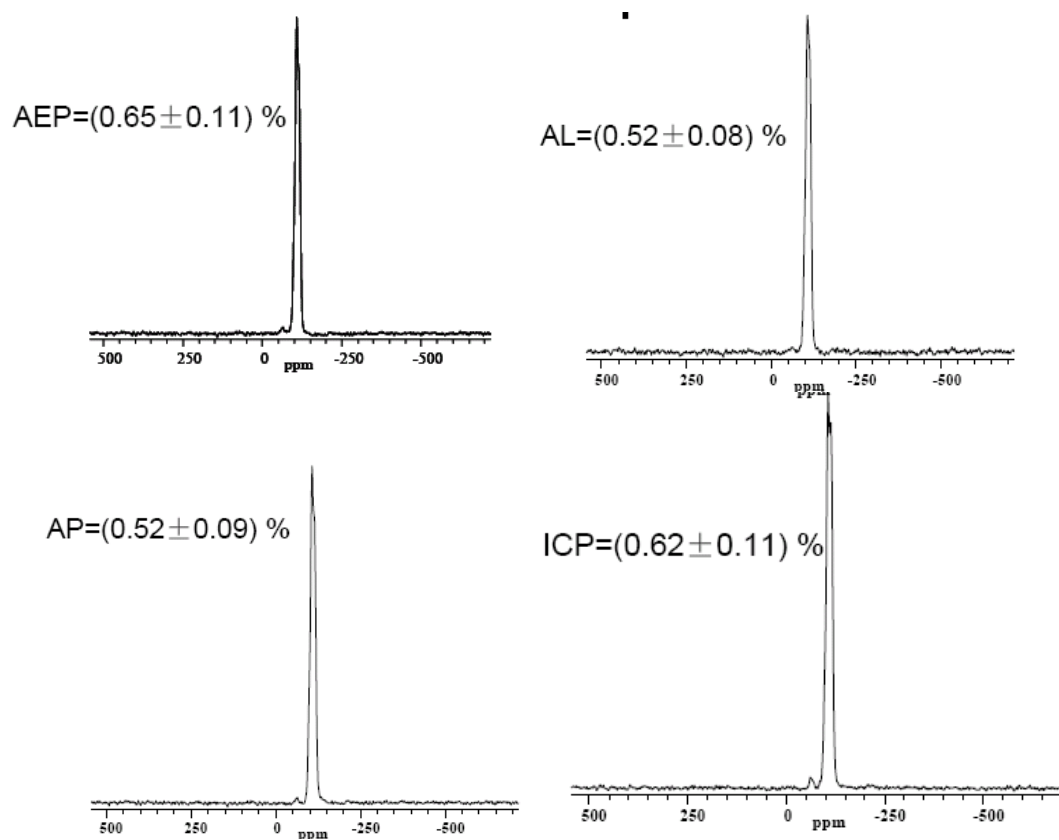**Figure3.** ^{1}H-^{29}Si DPMAS spectra of MCS

Figure4. ^{1}H-^{29}Si CPMAS spectra of MSN with FITC

CHAPTER 5. CONCLUSION

In this thesis, two new types of mixed oxide catalysts are for the biofuel applications are described. Solid-state NMR of ^{29}Si was used to characterize these materials.

1. The homogenous catalysts used for the transesterfication reaction of soybean oil to biodiesel, such as sodium methoxide, sodium hydroxide or potassium hydroxide, require extensive post-treatment. A novel mesoporous calcium silicate was recently synthesized in Dr. Lin's group, which served as a highly recyclable heterogeneous catalyst for the transesterfication reaction in soybean oil and poultry fat. However, the reaction kinetics was too slow for practical applications. Here, we reported on a non-porous calcium silicate, which improved the reaction kinetics by a factor of six. It can be recycled 9 times with an average losing rate of 4 percent in activity for SBO and 3 times without decrease in activity for poultry fat. The synthesis process of this non-porous catalyst does not require the use of surfactant and calcination process, which makes it environmentally friendly and economically efficient.

2. The second mixed oxide catalyst was prepared for the selective synthesis of ethanol from syngas. The rhodium-based catalysts, which can be very efficient in this reaction, are often promoted by manganese. The traditional co-impregnation of Rh and Mn onto a support (e.g. SiO_2) has two main drawbacks. First, the Rh particles can be partially blocked by Mn, which reduces the accessible Rh surface. Second, Mn may become isolated from the Rh particles. To eliminate both possibilities, we have synthesized a mesoporous manganese oxide and used it as a support for Rh. The catalyst, which operates best at 310 ^{o}C, proved to be more efficient than the previously used co-impregnated Rh-Mn/SiO_2 and the Rh/SiO_2 catalysts.

3. The solid-state ^{29}Si NMR was used to calculate the Ca/Si ratio in the calcium silica catalysts and to quantify the functionalization of the silica materials with FTIC.

ACKNOWLEDGEMENTS

I would like to take this opportunity to express my sincere thanks to those who helped me with various aspects of conducting the research and the writing of this thesis. First and foremost, I thank Dr. Victor Lin and Dr. Pruski for their help, guidance, patience and support throughout this research and the writing of this thesis. Their insights and words of encouragement have often inspired me and renewed my hopes for completing my graduate education. Second, I would also like to thank my committee member, Dr. Fang for his efforts and contributions to this work. Last but not least, I would like to thank all the members in both Dr. Lin and Dr. Pruski' groups. Without their help, cooperation and support, I could not finish the research and thesis.